Growth and Frequency Pushing Effects in Relativistic Magnetron Phase-Locking

S.C. Chen

Plasma Fusion Center
Massachusetts Institute of Technology, Cambridge, MA 02139

ABSTRACT

A magnetron-specific phase-locking model has been developed using the standard equivalent-circuit approach which takes into account the unconventional magnetron growth characteristics as well as the frequency pushing effect. These effects owe their origin to the highly nonlinear electron-wave interaction, thus are believed to be more pronounced in relativistic magnetrons. The model predicts a wider locking-bandwidth and a shorter locking time than those in conventional locking theory. The phase-locked amplitude resonance occurs, as the results indicate, at an injection frequency different from that of the free-running oscillator.

1. INTRODUCTION

The past ten years have seen the rapid progress made in the research on high power microwaves.[1-3] Phase control of high power oscillators appears to be the logical and the promising means for harnessing and enhancing the unprecedented power output.[4-6] The relativistic magnetron, with its reentrant nature and high efficiency, is an especially desirable candidate as the heart of a phase-locked system.[7-9] The successful phase control of an ensemble of high power oscillators will have important applications in areas like radars, high-gradient acceleration of particles, and microwave power transmission. Research in this area has been very active[10-15] and major results were achieved recently in a short-pulse experiment.[10] Long-pulse operation[11-14 20] and the subsequent phase-locking[15] of relativistic magnetrons, provide more interesting application possibilities and involve greater technical challenges not encountered in the short-pulse experiments.

Conventional magnetrons have been successfully phase-locked for forty years, and the canonical van der Pol oscillator model[16] together with the Adler's locking criterion[17] have been adequate in understanding the phase-locking performance. These models, however, may not be suitable for the phase-locking of relativistic magnetrons for the following reasons: (1) Frequency pushing effect, namely the variation of frequency of oscillation with electrode current, was studied theoretically and found to affect the phase-locking behaviour in nonlinear oscillators provided the magnitude of the frequency pushing is large enough. [18,19] It is believed that the high current involved in the relativistic magnetrons will result in a more pronounced frequency pushing effect, although the magnitude has not been carefully documented experimentally. Recently, frequency tuning with changes in operating fields was observed in some experiments,[20,21] which begin to shed light on the magnitude of the frequency pushing in relativistic magnetrons. (2) Phase locking of pulsed oscillators — especially those with a cavity fill time comparable with the pulse length — requires attention to the details of the magnetron growth process.

A good model for the phase-locking of pulsed relativistic magnetrons, therefore, should contain the frequency pushing effect and the magnetron growth model. The ubiquitous van der Pol equation[16] lacks both; hence will not serve the purpose of a magnetron model equation. Moreoverr, it is well known that the growth and frequency characteristics (or, equivalently, the dispersion relation) cannot be calculated easily from first principles for magnetrons. This is prohibited by the highly nonlinear crossed-field interaction in magnetrons and the complex geometry and particle dynamics involved. It is the purpose of this paper to temporarily de-emphasize the differences between the relativistic and the conventional magnetrons (except for noting the difference in magnitude of the frequency pushing effect), and to apply the conceptually simple approach — modelling the growth and frequency features within the lumped-circuit model — to obtain fundamental understanding of the phase-locking behavior in magnetrons.

Section 2 justifies the choice of model equations for the electronic conductance and susceptance used in the equivalent-circuit model using two independent simulation techniques, and discusses the relevant features in the operation of free-running magnetrons. In section 3, phase locking with weak injection near the oscillator frequency is analyzed. Important effects due to the magnetron–specific features are identified.

2. SIGNAL GROWTH AND FREQUENCY-PUSHING IN MAGNETRONS

The distinct features that set magnetrons apart from other oscillators are its the growth and saturation characteristics. This is illustrated qualitatively in Figure 1, in which the electronic conductance g (the ratio of RF current and RF voltage) is plotted against the RF voltage.[22,23] The conductance curve for magnetrons (Figure 1a) assumes a "concave" shape with a second derivative greater than zero. This phenomenon, namely the existence of finite RF current even with very small RF voltage, has long been observed in magnetron operation.[22,23] The state of zero current is extremely unstable which, with very small perturbation, breaks into a state of large current. This behavior, which differs drastically from that of most conventional self-excited oscillators (Figure 1b), leads to some unique properties in magnetrons to be described in the following.

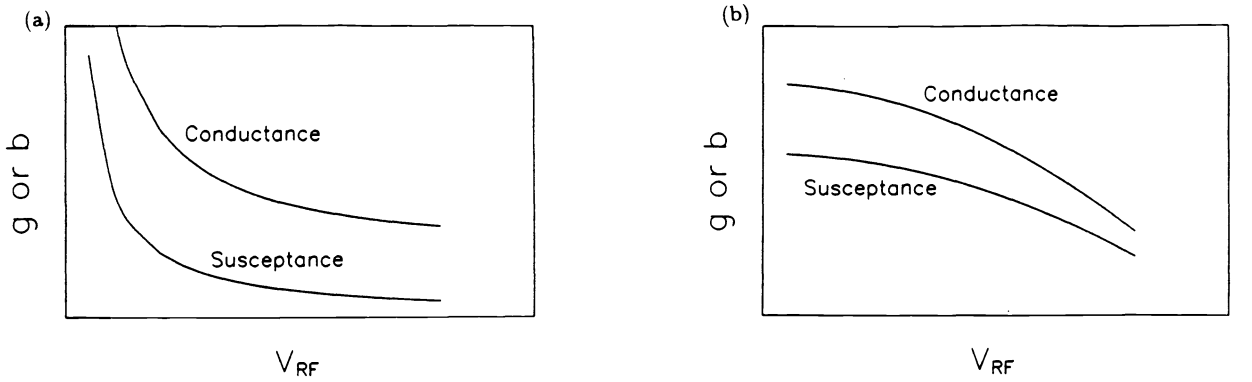

Figure 1 Electronic conductance g and susceptance b as functions of the rms voltage in the RF-field for (a) magnetrons, and (b) conventional regenerative oscillators.

To model this magnetron feature, Slater[22,23] suggested using

$$g = \frac{1}{R}\left(\frac{V_{DC}}{V_{RF}} - 1\right) \tag{1}$$

to relate the conductance to the rms RF-voltage (see Figure 1a). This is to be compared with the more conventional expression for other oscillators (Figure 1b)

$$g = g_0\left(1 - \frac{{V_{RF}}^2}{{V_{DC}}^2}\right), \tag{2}$$

where g_0 is the small-signal gain. It can be shown that Eq. (2), which can often be derived from first principles for simpler oscillators,leads to the van der Pol oscillator equation. [16]

In addition to the in-phase component of the RF current which governs the temporal growth, of equal importance is the contribution from the out-of-phase RF current which determines the output frequency. Frequency-pushing, namely the frequency change caused by the presence of the electron space charge — the same space charge responsible for the gain —, is modeled by the following expression[22,23]

$$b = b_0 - g \cdot tan\alpha. \tag{3}.$$

The relationship between the real and imaginary parts of the frequency (susceptance b and conductance g) is evident from Figure 1. It should not be surprising that the frequency pushing effect, represented by the pushing parameter α of order unity, plays an important role in magnetron phase locking since the angle α characterizes the phase lag between the electron bunch (spoke in magnetrons) and the resonant wave. In simple devices like reflex klystrons, the angle α is found to be the deviation of the average transit-time from $\frac{2}{3}\pi$ (for $1\frac{3}{4}$-mode) in the repeller region.[23]

To justify the choice of the model equation (1), we have[24] extended an existing semi-empirical model of conventional magnetrons[25–29] and applied the model to examine the behavior of the electronic conductance. We have developed a computer program based on this model and applied it to the 4J50 magnetron (high power X-band, see Vaughan[25] for tube parameters). By changing the loading level at the output, the corresponding operating RF-amplitudes under steady-state condition were monitored. The result is shown in Figure 2a. We have[24] successfully reproduced the gain characteristics (Figure 2a) described by Eq. (1).

A second approach was taken by Dombrowsky[30] using a more elaborate simulation scheme.[31] The result of the simulation for magnetron 2J32 is shown in Figure 2b.

The spoke model[24] and the Dombrowski simulation[30] thus provide independent means of confirming the $1/V_{RF}$ dependence of the magnetron growth.

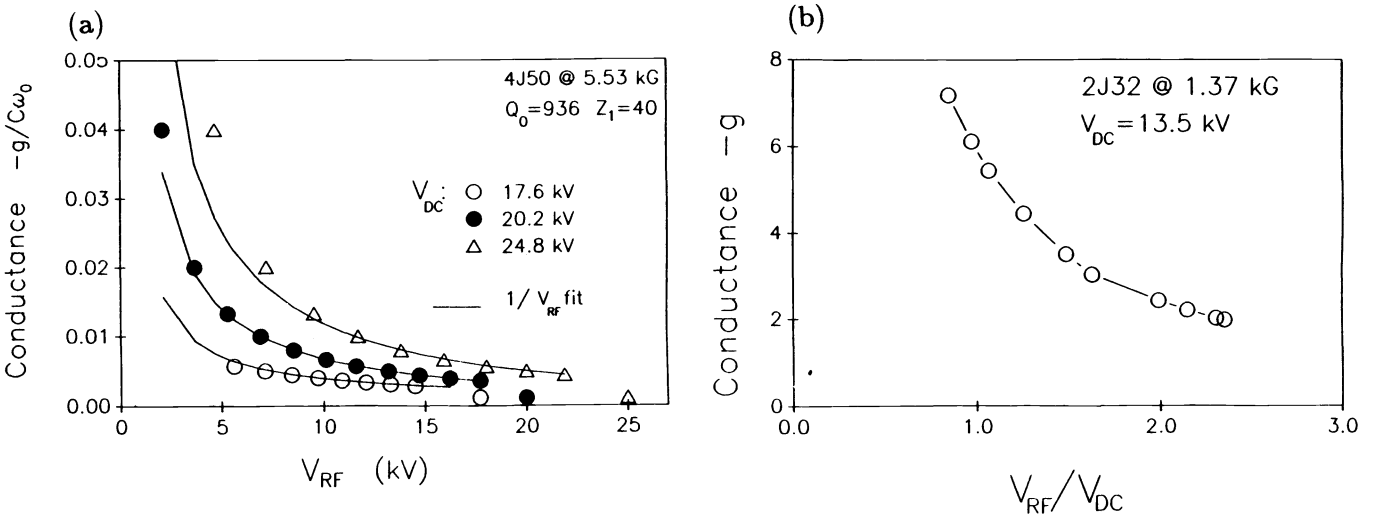

Figure 2 Calculated magnetron electronic conductance g as a function of V_{RF}. (a) The 4J50 magnetron operating at steady-state with three different DC-voltages are calculated using macro-spoke model (Chen). (b) The 2J32 magnetron starting up from injected noise is calculated using macro-particle simulation (Dombrowski). Both (a) and (b) produced the g–dependance described by the model equation (1).

Based on the magnetron-specific models for g and b described in Eqs. (1) and (3), we then proceed to construct an equivalent-circuit model and study the steady-state and the phase-locking operation in magnetrons and relativistic magnetrons.

The model is based upon the general oscillator equation derived from the standard parallel RLC circuit[22,23] (see Figure 3). We follow the techniques and notations used in references 22, and 23. The magnetron gain mechanism is represented by a shunt electronic admittance $g + ib$. The single-mode oscillator equation for this circuit is

$$\frac{g+ib}{C\omega_0} = i\left(\frac{\omega}{\omega_0} - \frac{\omega_0}{\omega}\right) + \frac{1}{Q_0} + \frac{G+iB}{Q_{ext}}, \tag{4}$$

where $G + iB$ is the voltage-dependant nonlinear complex admittance of the load. In the equation, ω is the output frequency, $\omega_0 = \frac{1}{\sqrt{LC}}$, $Q_0 = RC\omega_0$, and Q_{ext} is the external Q.

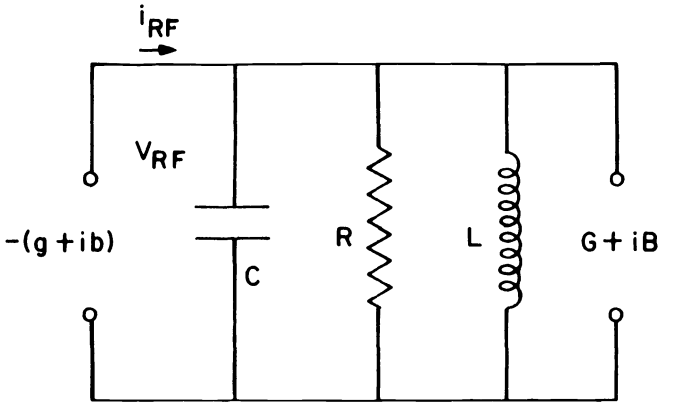

Figure 3 Equivalent circuit used in modelling magnetron operation. $g+ib$ is the complex admittance describing the electron-wave interaction. $G+iB$ represents the load admittance. RLC-circuit models the magnetron resonance cavity with loss.

Inserting Eqs. (1) and (3) into Eq. (4), and separating the real and imaginary parts, the steady-state values of the amplitude V_{RF0} and frequency ω' for a free running magnetron are found to be[22,23]

$$V_{RF0} = \frac{V_{DC}}{2RC} \frac{1}{\frac{1}{2}\omega_0(\frac{1}{Q_L} + \frac{1}{RC\omega_0})} \tag{5},$$

and

$$\omega' = \omega_0 + \frac{1}{2}(\frac{b_0}{C} - \frac{B\omega_0}{Q_{ext}}) - \frac{\omega_0 \cdot tan\alpha}{2Q_L}. \tag{6}$$

Eq. (6) contains both the frequency pulling ($\frac{B\omega_0}{Q_{ext}}$) as well as the pushing $\frac{\omega_0 \cdot tan\alpha}{2Q_L}$ terms. We define a growth parameter

$$\gamma = \frac{1}{2}\omega_0(\frac{1}{Q_L} + \frac{1}{RC\omega_0}) \tag{7}$$

for later convenience.

The amplitude and frequency evolution in the magnetron start-up phase can be calculated under situations when the frequency is much greater than the growth rate $\omega \gg \gamma$, hence the growth process can be approximated adiabatically by a succession of instantaneous steady-state solutions.[22,23] The oscillator equation is then modified by the addition of a temporal growth rate $-i\Gamma(t)$ to the frequency ω

$$\frac{g+ib}{C\omega_0} = i(\frac{\omega - i\Gamma}{\omega_0} - \frac{\omega_0}{\omega - i\Gamma}) + \frac{1}{Q_0} + \frac{G+iB}{Q_{ext}}, \tag{8}$$

where

$$\Gamma(t) = \frac{\dot{V}_{RF}}{V_{RF}}. \tag{9}$$

The real part of Eq. (8) again governs the growth

$$\frac{g}{C\omega_0} = \frac{1}{Q_L} + \frac{2}{\omega_0}\Gamma(t). \tag{10}$$

Inserting Eq. (1) into Eq. (10) and using the definition of Γ in Eq. (9), one obtains the RF amplitude equation

$$\dot{V}_{RF} = -\gamma \cdot (1 - \frac{V_{RF0}}{V_{RF}}) \cdot V_{RF}. \tag{11}$$

The solution of Eq. (11) gives the RF amplitude evolution in magnetrons

$$V_{\rm RF}(t) = V_{RF0} \cdot (1 - \eta e^{-\gamma t}), \tag{12}$$

where

$$\eta = 1 - \frac{V_i}{V_{RF0}} \sim 1 \tag{13}$$

characterizes the initial signal level in the tube. The interesting implication is that the stage of starting from noise is rapidly passed through, and a linear (not exponential) build-up then brings the system to saturation in a manner similar to a capacitor charging up. The detail mechanism behind these observations for magnetrons, however, remains largely unexplored.

Solving the equation obtained by taking the imaginary part of Eq. (8), one finds that the output frequency evolves according to

$$\omega(t) = \omega' - tan\alpha \cdot \gamma \cdot \frac{\eta e^{-\gamma t}}{1 - \eta e^{-\gamma t}}, \tag{14}$$

and approaches the steady-state free running frequency ω' defined in Eq. (6).

3. PHASE LOCKING OF RELATIVISTIC MAGNETRONS

The choice of (g, b), which contains the interaction physics, determines the oscillator-specific phase-locking behavior. It is obvious that the deviation of Eq. (1) from (2), and the choice of nonzero frequency pushing parameter in our magnetron model, will lead to new effects which are absent in conventional phase locking model based on Eq. (2) and no frequency pushing. We follow the techniques developed in previous work[22,23,32,33] and treat the locking source as part of the magnetron load which injects counter propagating I_1 and V_1 at a frequency ω_1. The driven oscillator equation becomes

$$\frac{g + ib}{c\omega_0} = i(\frac{\omega}{\omega_0} - \frac{\omega_0}{\omega}) + \frac{1}{Q_0} + \frac{G + iB + 2\rho e^{-i[\phi - (\omega_1 t + \theta_i)]}}{Q_{ext}}. \tag{15}$$

In Eq. (15), the injection parameter ρ , the injection phase θ_i, and the relative phase θ are defined as follows:

$$\rho = \frac{1}{2}(\frac{V_1}{V} - \frac{I_1}{I}) \cdot \sqrt{G^2 + B^2} \tag{16}$$

$$\theta_i = sin^{-1} \frac{B}{\sqrt{G^2 + B^2}} \tag{17}$$

$$\theta(t) = \phi_{Mag}(t) - (\omega_1 t + \theta_i). \tag{18}$$

Separating the real and imaginary parts, we have

$$\frac{g}{c\omega_0} = \frac{1}{Q_L} + \frac{2\rho cos\theta}{Q_{ext}} \tag{19}$$

$$\frac{b}{c\omega_0} = \frac{2(\omega - \omega_0)}{\omega_0} + \frac{B}{Q_{ext}} - \frac{2\rho sin\theta}{Q_{ext}}. \tag{20}$$

In deriving (20), we have assumed $\omega \sim \omega_0$ for simplicity.

It is interesting to point out that although the magnetron-specific conductance and susceptance Eqs. (1) and (3) were repetitively described and emphasized in Slater's work[22,23], they were not included in his phase locking calculations.[22] Here we introduce Eqs. (1) and (3) into Eqs. (19) and (20) , and obtain the equations for driven magnetrons. The equations governing the amplitude and the frequency of the steady-state are

$$V_{\rm RF} = V_{RF0}\frac{1}{1+\frac{\rho\omega_0 cos\theta}{Q_{ext}\gamma}} \tag{21}$$

and

$$\omega - \omega' = \frac{\rho\omega_0}{Q_{ext}}(sin\theta - cos\theta \cdot tan\alpha), \tag{22}$$

where V_{RF0} and ω' are the free-running amplitude and frequency defined in Eqs. (5) and (6). To simplify the equations, we normalize all frequencies with respect to ω_0 and introduce the dimensionless injection and detuning parameters into Eqs. (21) and (22)

$$\mu = \frac{\rho}{Q_{ext}}, \quad \sigma = \frac{\omega' - \omega_1}{\omega_0}. \tag{23}$$

The resultant equations

$$V_{\rm RF} = V_{\rm RF}(\theta) = V_{RF0}\frac{1}{(1+\frac{\mu}{\gamma}\cos\theta)}, \tag{24}$$

and

$$\frac{1}{\omega_0}\frac{d\theta}{dt} = \frac{\mu}{\mid cos\alpha \mid} sin(\theta - \alpha) + \sigma \tag{25}$$

describe the amplitude and the relative phase evolution. It is important to realize the parameter range in which the analysis is valid. The assumptions we have made so far can be conveniently collected in terms of a simple inequality which relates frequency, growth parameter, injection amplitude, pushing parameter, and frequency difference:

$$1 = \omega_0 > \gamma \geq \frac{\mu}{\mid cos\alpha \mid} \geq \mid \sigma \mid . \tag{26}$$

The condition under which phase locking occurs is obtained by setting Eq. (25) to zero for steady-state,

$$\frac{\mu}{\mid cos\alpha \mid} \geq \mid \sigma \mid, \tag{27}$$

which reduces to the familiar Adler's condition[17] $\mu \geq \mid \sigma \mid$ when the frequency pushing parameter α is zero. The widening of the locking frequency range can be quite appreciable depending on the amount of frequency pushing (see Table I). The experimentally observed magnitude of α for conventional magnetrons ranges roughly from 0 to 1.5 depending on the operating DC voltage. Under normal operating condition, it is on the low side. An α of 0.25 is chosen as the typical value for conventional magnetrons and is used in the following analysis. The high anode current, typically 1 kA in relativistic magnetron operation, is expected to give rise to even larger α's (Table I).

The final relative phase of the locked system is also modified by the nonzero pushing parameter α (Table I)

$$\theta_{lock} = sin^{-1}(-\frac{\sigma \mid cos\alpha \mid}{\mu}) + \alpha. \tag{28}$$

To summarize the steady-state behavior of the weak injection phase locking system near the fundamental locking zone, we combine the phase and amplitude equations (24) and (25) by cancelling the θ–dependance. The resultant equation

$$\frac{(\frac{V_{\rm RF}}{V_{RF0}} - 1)^2}{(\frac{\mu}{\gamma})^2} = (\pm\sqrt{1 - (\frac{\sigma}{\mu'})^2}\, cos\alpha + \frac{\sigma}{\mu'} sin\alpha)^2 \tag{29}$$

contains the dependance of output amplitude $V_{\rm RF}$ on three parameters: the injection parameter $\mu' = \mu/\mid cos\alpha \mid$, the pushing parameter α, and the detuning parameter σ. The effect of the frequency pushing can be singled out by comparing the above equation with the case when $\alpha = 0$

$$\frac{(\frac{V_{\rm RF}}{V_{RF0}} - 1)^2}{(\frac{\mu}{\gamma})^2} + \frac{\sigma^2}{\mu^2} = 1\ , \qquad \alpha = 0. \tag{30}$$

Figure 4 illustrates this comparison by showing the loci of the steady phase-locked states on the σ–V_{RF} plane for $\gamma = 0.1$. Different curves correspond to different values of injection amplitudes μ. Figure 4 depicts the dependance of V_{RF} on σ for the case of (a) no frequency pushing ($\alpha = 0$), and (b) finite frequency pushing ($\alpha = 0.25$). The free-running state is represented by the point $\sigma = 0, V_{RF}/V_{RF0} = 1$. It is clearly seen in Figure 4a, that the loci of the phase locked states for weak injection form a family of "ellipses" with an eccentricity $\epsilon = \sqrt{1-\gamma^2}$. The deviation of the "ellipses" from exact elliptical shape is caused by the unconventional form of the growth model (1); the results obtained for conventional oscillators based on (2) form evenly spaced ellipses with a common geometric center. Characterized by an injection parameter μ, each ellipse in Figure 4 consists of two branches. The result of a stability analysis established the existence of a stability criteria ($\cos\theta_{lock} \leq 0$), shown in Figure 4 as the dashed line. Only the upper branch of the double-valued ellipses constitutes the stable solutions.

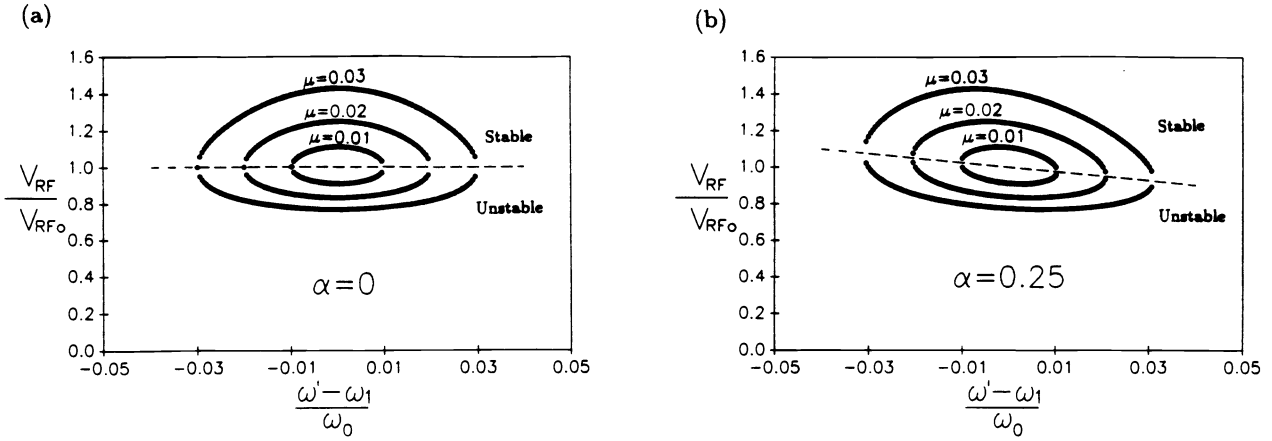

Figure 4 Amplitude ($\frac{V_{RF}}{V_{RF0}}$) versus normalized frequency difference σ in the phase-locked states for three injection amplitudes $\mu = 0.01, 0.02, 0.03$. (a) No frequency pushing, each ellipse corresponds to an injection parameter μ. (b) The effect of frequency pushing ($\alpha = 0.25$) rotates the ellipses and results in a wider locking bandwidth and a shifted amplitude resonance frequency.

A nonzero α deforms the ellipses in a complex way (Figure 4b) . In phase-locked states, the frequency pushing effectively rotates the ellipses by an angle

$$\theta_1 = tan^{-1}(\gamma\ sin\alpha), \tag{31}$$

which results in a wider locking bandwidth, as described by (27), than the conventional Adler's condition (see Table I for numerical examples). The maximum power output, that is, the amplitude resonance, occurs at an injection frequency detuned from the free-running value

$$\sigma_m = \mu\ sin\alpha, \tag{32}$$

or equivalently the resonance frequency ω_r is

$$\omega_r = \omega_1 + \frac{\rho}{Q_{ext}} sin\alpha. \tag{33}$$

The amount of detuning, namely the difference of the optimal injection frequency and the free-running frequency, can become appreciable with large μ (Table I).

TABLE I.

Pushing Parameter α	Locking Bandwidth†	Resonant Frequency Shift‡	Locked Phase*	Locking Time** (RF Cycles) $\theta \leq 2°$	$\theta \leq 0.1°$
0	1	0%	−90°	306	477
0.25	1.03	0.5%	−61°	244	405
0.50	1.14	1%	−33°	171	315
1.00	1.85	1.7%	+25°	87	171
1.25	3.17	1.9%	+53°	63	111

† in $\frac{\rho\omega_0}{Q_{ext}}$

‡ % of free running frequency, for the case $\mu = 0.02$

* for phase locking at the edge of the Adler locking band ($\sigma = \mu$)

** $\sigma = 0.5\mu$, $\theta_i = \theta_{locked} + \frac{\pi}{2}$

The boundary between the stable and the unstable branches, shown in Figure 4 as the dashed line, due to the non rigid body defromation, is tilted by a different angle

$$\theta_2 = tan^{-1}\frac{sin2\alpha}{2\gamma(1-(\frac{\mu sin\alpha}{\gamma})^2)} \sim tan^{-1}\frac{sin2\alpha}{2\gamma}. \tag{34}$$

The tilting effectively makes the phase-locked power output asymmetrical with respect to the injection frequency.

Transient behavior is of special interest in the case of phase-locking pulsed oscillators. The transient solution for the locking process is obtained by integrating Eq. (25) with respect to time. For the locking case ($\sigma < \mu'$), the relative phase evolves according to

$$\theta(t) = 2\ tan^{-1}(-\frac{\mu'}{\sigma} + \frac{A}{\sigma}\frac{1+De^{At}}{1-De^{At}}) + \alpha, \tag{35}$$

where

$$A = \sqrt{\mu'^2 - \sigma^2} \tag{36}$$

is the inverse of characteristic time and

$$D = \frac{\sigma\ tan\frac{-\theta_i-\alpha}{2} + \mu' - A}{\sigma\ tan\frac{-\theta_i-\alpha}{2} + \mu' + A} \tag{37}$$

is the parameter characterizing the amplitude of the transient. It is easily shown that $\theta(0) = -\theta_i$, and $\theta(\infty) = \theta_{lock}$. As (35) indicates, phase locking is a continuous process which occurs on a time scale T_{lock}. The locking time T_{lock} is a function of (A,D), which in turn depends on the parameter set $(\mu, \sigma, \alpha, \theta_i)$. Using (35)–(37), it can be proved, and has been demonstrated by numerical examples in Table I, that the frequency pushing effect ($\alpha \neq 0$) shortens the locking time (independent of the sign of α) !

For the unlocked case ($\sigma > \mu'$), the relative phase evolves according to

$$\theta(t) = 2\ tan^{-1}(\frac{A'q + (\mu'q+\sigma)\cdot tan\frac{A'}{2}t}{A'q - (\sigma q+\mu')\cdot tan\frac{A'}{2}t}) + \alpha, \tag{38}$$

where

$$A' = \sqrt{\sigma^2 - \mu'^2}, \tag{39}$$

and

$$q = tan\frac{-\theta_i - \alpha}{2}. \tag{40}$$

In the extreme case when the two frequencies are far apart ($\mu' \ll \sigma$), simple beating is recovered

$$\theta(t) = -\theta_i + \sigma \cdot t. \tag{41}$$

4. CONCLUSIONS

We have constructed a magnetron-specific equivalent-circuit model for the study of the steady-state and the phase-locked operation in magnetron oscillators. The unconventional magnetron growth characteristics lead us to believe that the state of pre-oscillation equilibrium is extremely unstable which, with very small perturbation, breaks into a state of large RF current. The magnetron growth process rapidly passes through the stage of starting up from noise, followed by a linear (not exponential) build-up which then brings the system to saturation. More theoretical effort is needed to explain the phenomena.

Besides the growth characteristics, the frequency pushing manifests itself in many effects in magnetron phase-locking which may be important for relativistic magnetrons operating with high anode currents. Specifically: the locking bandwidth is wider than the usual Adler's condition; the resonance of the phase-locked amplitude occurs at an injection frequency different from the free-running frequency; the time required for locking to occur is shortened by the frequency pushing effect; and the relative phase of the locked-state is modified by the pushing parameter.

Recently, the importance of the frequency pushing effect on the phase locking of regenerative oscillators has also been identified theoretically and studied by modeling the nonlinear frequency shift with a Duffing (cubic restoring force) term in a van der Pol oscillator.[18,19] The connection between the two frequency pushing effect models — namely the van der Pol/Duffing oscillator and the magnetron equivalent circuit model — is currently under study. It is also possible to construct a magnetron-oscillator differential equation containing both the growth and the frequency features, which will be applied to the modelling of general magnetron related phenomena on the oscillation time scale.

5. Acknowledgement

I am grateful to G. Bekefi, R.C. Davidson, G.L. Johnston, and R. Temkin for very useful discussions. This work was supported by SDIO/IST, and managed by Harry Diamond Laboratories.

6. REFERENCE

1. V.L. Granatstein and I.A. Alexeff, Editors, *High Power Microwave Sources*, Artech House (1987).

2. N. Rostoker, Editor, *Microwave and Particle Beam Sources and Propagation*, Proc. SPIE 873 (1988).

3. H.E. Brandt, Editor, *Microwave and Particle Beam Sources and Directed Energy Concepts*, Proc. SPIE 1061 (1989).

4. D. Price, H. Sze, and D. Fittinghoff, *J. Appl. Phys.* **65**, 5185 (1989).

5. A.W. Fliflet and W.M. Manheimer,*Phys. Rev. A* **39**, 3432 (1989).

6. W. Woo, J. Benford, D., Fittinghoff, B. Harteneck, D. Price, R. Smith, and H. Sze, *J. Appl. Phys.* **65**, 861 (1989).

7. W.C. Brown,*IEEE Trans. MTT*, **MTT-21**, 753 (1973).

8. P.B. Wilson, SLAC Pub. 4803, Dec. (1988).

9. T. Overett, D.B. Remsen, E. Bowles, G.E. Thomas, and R.E. Smith, III, IEEE Particle Accelerator Conf., 1464 (1987).

10. J. Benford, H.M. Sze, W. Woo, R.R. Smith, and B. Harteneck , *Phys. Rev Lett.*, **62**, 969 (1989).

11. S.C. Chen and G. Bekefi, "Relativistic Magnetron Research", N. Rostoker, Editor, Proc. SPIE **873**, 18 (1988).

12. A.G. Nokonov, I.M. Roife, Yu.M. Savel'ev, and V.I. Engel'ko, *Sov. Tech. Phys.* **32**, 50 (1987).

13. A.N. Didenko, A.S. Sulakshin, G.P. Fomenko, V.I. Tsvetkov, Yu. G. Shtein, and Yu.G.Yushkov, *Sov. Tech. Phys. Lett.* **4**, 331 (1979).

14. I.Z. Gleizer, A.N. Didenko, A.S. Sulakshin, G.P. Fomenko, and V.I. Tsvetkov, *Sov. Tech. Phys. Lett.* **6**, 19 (1980).

15. S.C. Chen, G. Bekefi, R. Temkin, and C. de Graff, "Proposed Injection Locking of a Long Pulse Relativistic Magnetron", H.E. Brandt, Editor, Proc. SPIE **1061**, 157 (1989).

16. B. van der Pol, *Phil. Mag.* S. 7. **3**, No.13 (1927).

17. R. Adler, Proc. IRE **34**, 351 (1946).

18. J.E. Walsh, G.L. Johnston, R.C. Davidson, and D.J. Sullivan, SPIE Proceedings **1061**, 161 (1989).

19. H. Lashinsky, Periodic Nonlinear Phenomena, unpublished manuscript.

20 S.C. Chen, G.Bekefi, and R. Temkin, "The operation of a long pulse relativistic magnetron in a phase-locking system" , in this volumn.

21. I.I. Vintizenko, A.S. Sulakshin, and G.P. Fomenko, *Sov. Tech. Phys. Lett.*, **13**, 579 (1987).

22. J.C. Slater, R.L.E. Technical Report No. 35, M I T (1947).

23. J.C. Slater, *Microwave Electronics* (1954).

24. S.C. Chen, G. Bekefi, and D.P. Aalberts, unpublished.

25. J. R. M. Vaughan, IEEE Trans. Electron Devices **ED-20**, 818 (1973); J. R. M. Vaughan, IEEE Trans. Electron Devices, **ED-21**, 132 (1974).

26. A. Azumi, *Fujitsu Sci. Tech. J.*, **7**, 85 (1971).

27. J. F. Hull, *IRE Trans. Electron Devices*, **ED-8** 309 (1961).

28. J. F. Hull, Ph.D. dissertation, Polytechnic Institute of Brooklyn (1958).

29. H. W. Welch, *Proc. IRE* **41**, 11 (1953).

30. G.E. Dombrowski, private communication.

31. G.E. Dombrowski, IEEE Trans. Electron Devices, **ED-35**, 2060 (1988).

32. E.E. David, R.L.E. Technical Report No. 100, MIT (1949).

33. E.E. David, in *Crossed Field Microwave Devices*, Vol.2, E. Okress Ed. p.375 (1961).